

## Bonding in and Gas-phase Pyrolysis of the Arsoranes and Stibanes $\text{EMe}_3\text{X}_2$ (E = As or Sb, X = F or Cl) and $\text{SbMe}_4\text{F}$ : Ultraviolet Photoelectron and Field-ionization Mass Spectrometric Studies †

Susanne Elbel\*

*Institut für Anorganische und Angewandte Chemie der Universität Hamburg, Martin-Luther-King-Platz 6, D-2000 Hamburg 13, Federal Republic of Germany*

Helge Egsgaard and Lars Carlsen\*

*Chemistry Department, Risø National Laboratory, DK 4000 Roskilde, Denmark*

The He I (and partially He II) photoelectron spectra of the gaseous Group 5 molecules  $\text{AsMe}_3\text{F}_2$ ,  $\text{AsMe}_3\text{Cl}_2$ ,  $\text{SbMe}_3\text{F}_2$ ,  $\text{SbMe}_3\text{Cl}_2$ , and  $\text{SbMe}_4\text{F}$  are presented and assigned using the known ionization potentials of  $\text{SbMe}_3$  and  $\text{EMe}_3$  (E = As or Sb) and simple molecular-orbital models. Calculations have been performed for the series  $\text{AsH}_3$ ,  $\text{AsH}_5$ ,  $\text{AsH}_3\text{F}_2$  using the SCC-X $\alpha$  method. Upon pyrolysis both  $\text{AsMe}_3\text{Cl}_2$  and  $\text{SbMe}_3\text{Cl}_2$  undergo unimolecular elimination of HCl in the gaseous phase, indicating the intermediacy of new transient species ' $\text{EMe}_3\text{Cl}_2 - n\text{HCl}$ .' However, reductive elimination of MeF is favoured by the gaseous fluorides. These results are strongly supported by high-temperature field-ionization mass spectrometry under similar conditions. Loss of HCl was also observed during solid-state pyrolysis of ionic  $\text{PMe}_3\text{Cl}_2$  *in vacuo*.

The present study is an extension of earlier work on the photoelectron (p.e.) spectra of volatile pentavalent Group 5 compounds.<sup>1,†</sup> These species have intrigued theoreticians, spectroscopists, and preparative chemists for decades.<sup>2,3</sup> However, definite answers to problems associated with ligand scrambling,<sup>2,4</sup> *d*-orbital participation,<sup>3b,5</sup> bond ionicity or ligand apicophilicity<sup>6</sup> and with the mode of reductive elimination<sup>2a,7a</sup> are still pending. Theoreticians often tend to simplify matters by referring to hypothetical hydrogenated prototypes which are introduced without any experimental justification even when alkyl homologues are missing,  $\text{PH}_5$  can be regarded as a typical example of this practice.<sup>7</sup> As pointed out earlier,<sup>1</sup> heavy-atom alkyl congeners, as far as they are experimentally observable, should be well suited to represent the lighter, mostly hypothetical homologues with respect to valence ionization-energy patterns, second-row derivatives being excluded.

In the present study the relative gas-phase ionization potentials (i.p.s) of  $\text{AsMe}_3\text{F}_2$ ,  $\text{SbMe}_3\text{F}_2$ ,  $\text{AsMe}_3\text{Cl}_2$ ,  $\text{SbMe}_3\text{Cl}_2$ ,<sup>1</sup> the latter being included for consistency, and  $\text{SbMe}_4\text{F}$  are treated within the frame of qualitative molecular-orbital (m.o.) interaction schemes using Grodzicki's SCC-X $\alpha$  method.<sup>8</sup> Apart from  $\text{PMe}_3\text{F}_2$ , these species lack volatile covalent phosphorane counterparts, but are expected to show ionization-energy patterns like those of the  $\text{EH}_3\text{X}_2$  (E = Group 5 element, X = halide) or the  $\text{PMe}_3\text{X}_2$  homologues.

### Experimental

The He I and He II p.e. spectra of  $\text{AsMe}_3\text{F}_2$ ,  $\text{SbMe}_3\text{F}_2$ , and  $\text{SbMe}_4\text{F}$  were recorded on a 0078 Helectros PE spectrometer (H. J. Lempka, Beaconsfield) and were calibrated using the argon doublet and  $\text{He}^+$  lines. The He I spectra of the dichlorides were recorded at different temperatures using an UPG 200 PE spectrometer (Leybold-Heraeus, Cologne) and were calibrated with argon. The resolution was better than 25 meV for  $\text{AsMe}_3\text{F}_2$  and  $\text{EMe}_3\text{Cl}_2$ , but only 40–50 meV for  $\text{SbMe}_3\text{F}_2$  and  $\text{SbMe}_4\text{F}$  on both spectrometers. The ionization potentials are quoted to an estimated accuracy of  $\pm 0.10$  eV for

the former and  $\pm 0.15$  eV for the latter species. The heated inlet system used for the gas-phase pyrolysis studies was designed by J. Krizek (Leybold-Heraeus). Its construction is based on a commercial valve lock connected to a heatable sample rod with a sublimation chamber at the end (temperatures up to *ca.* 800 K). The sample vapour is pyrolysed on passing through a tungsten wire-wrapped molybdenum tube which can be heated up to *ca.* 1900 K by electron bombardment. The distance between the pyrolysis zone and ionization chamber is about 4–5 cm. The sample pressure ranged from  $5 \times 10^{-4}$  to  $10^{-5}$  mbar within the inlet tube and from  $10^{-6}$  to  $10^{-7}$  mbar within the analyser recipient.

Mass spectrometric investigations were carried out using a Varian MAT CH 5D double-focusing mass spectrometer equipped with a combined electron impact ionization (e.i.)–field ionization (f.i.)–field desorption (f.d.) ion source. The f.i. spectra were obtained using a 10- $\mu\text{m}$  tungsten wire, activated in benzonitrile vapour as emitter.

The pyrolyses were carried out by application of the low-pressure Curie-point pyrolysis technique, previously described in detail,<sup>9</sup> the pyrolysis products being introduced directly into the ion source of the mass spectrometer. In all cases gold-plated Curie-point pyrolysis filaments were used in order to eliminate possible surface-promoted reactions.<sup>10</sup> Pyrolyses were carried out at 1043 K.

Mass spectra of the undecomposed compounds were obtained using the direct-inlet probe.

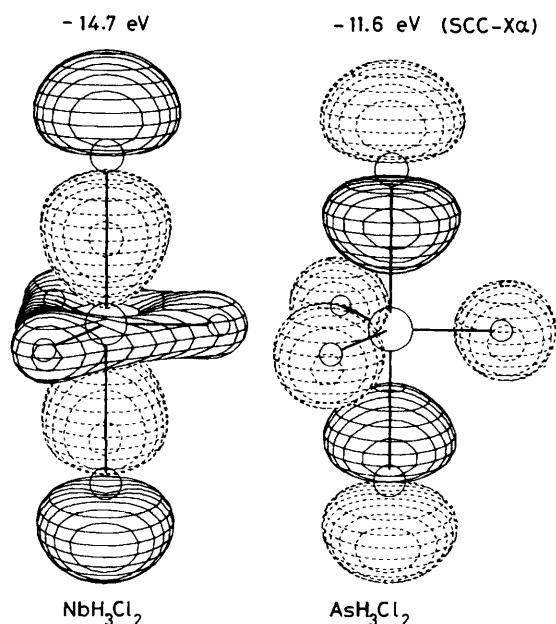
Model calculations were made for  $\text{AsH}_3$ ,  $\text{AsH}_5$ , and  $\text{AsH}_3\text{F}_2$  with and without central *d* atomic orbitals (a.o.s) in the basis set using the semiempirical SCC-X $\alpha$  method as described in recent papers.<sup>8</sup> Only valence electrons were taken into account. SCC-X $\alpha$  parameters for the elements were fitted on the basis of the known p.e. energies of  $\text{As}_2$ ,<sup>11</sup>  $\text{As}_4$ ,<sup>11</sup> and  $\text{F}_2$ .<sup>12</sup> Gas-phase geometries were taken from the literature (*cf.* ref. 8b) or were estimated ( $\text{AsH}_3\text{F}_2$ ,  $\text{AsH}_5$ ) from the bond-length variations which occur during the formal oxidative addition, *e.g.*  $\text{AsMe}_3 + \text{F}_2 \longrightarrow \text{AsMe}_3\text{F}_2$ ,<sup>13</sup> or as calculated by *ab initio* methods, *e.g.*  $\text{PH}_3 + \text{R}_2 \longrightarrow \text{PH}_3\text{R}_2$  (R = H or F).<sup>6,7</sup> The SCC-X $\alpha$  program was extended by the PSI/77 subroutines of Jorgensen<sup>14</sup> so as to plot the wavefunctions as presented in Figure 2. The compounds were prepared and purified as described previously.<sup>15–18</sup>

† Non-S.I. units employed: eV  $\approx 1.60 \times 10^{-19}$  J, bar =  $10^5$  Pa.

‡ The compound previously regarded as  $\text{SbMe}_3\text{FCl}$  is actually  $\text{SbMe}_3\text{F}_2$ .

## Results and Discussion

Except for  $\text{SbMe}_4\text{F}$  ( $C_{4v}$ ), all molecules under investigation are isosteric and belong to the  $D_{3h}$  point group. They possess 20 occupied valence m.o.s which transform as  $2e'' + 4e' + 3a_2'' + 1a_2' + 4a_1'$ . The five E-R  $\sigma$ -bonding m.o.s among them transform as  $1e' + 1a_2'' + 2a_1'$  and are directly related to those of virtual  $\text{EH}_5$  prototypes, as reported previously.<sup>2a,7,19</sup> The central atomic orbitals transform as  $s \rightarrow a_1'$ ,  $p \rightarrow a_2'' + e'$  ( $d \rightarrow a_1' + e' + e''$ ). It follows directly that one of the  $\sigma$ -type m.o.s, namely the lowest-energy  $a_1'$  m.o., is a non-bonding ligand m.o.s,  $n_{\text{R}}X_2$ , in the case of the main-group representatives where central  $d$  orbitals are generally regarded to be less important or even negligible. This particular m.o. type which should be subject to stabilization by the central atomic  $d_{z^2}$  ( $a_1'$ ) orbital is exemplified in Figure 3 for  $\text{AsH}_5$  (*cf.* the highest occupied molecular orbital, h.o.m.o.) with  $d$  a.o.s on the central atom and for  $\text{AsH}_3\text{Cl}_2$  ( $-d$ ) and  $\text{NbH}_3\text{Cl}_2$  ( $+d$ ) below. Here, the respective occupied  $3a_1'$  m.o.s are depicted to demonstrate the differing  $d$ -orbital effects for both types of compounds.



For symmetry and to a minor extent for energy reasons this ligand m.o. (see  $\text{AsH}_3\text{Cl}_2$  above) may additionally possess slight central  $s$  a.o. contributions, which are negligibly small as regards our m.o. calculations. There is experimental evidence from the Franck-Condon envelope of the first p.e. band of  $\text{SbMe}_5^1$  (see also Figure 2) that neither central  $d$  nor  $s$  a.o.s contribute much to this m.o. The band shape is characteristic for a pronounced  $0 \rightarrow 0$  vertical transition as is typical for ionizations from non-bonding m.o.s. This ligand m.o. is strongly stabilized for the transition-metal Group 5 counterparts as suggested by their p.e. spectra (*e.g.*  $\text{TaMe}_5$ ,  $\text{NbMe}_3\text{Cl}_2$ , or  $\text{TaMe}_3\text{Cl}_2$ )<sup>20</sup> and since this aspect has previously been extensively discussed<sup>1,20</sup> it will not be analysed in detail.

He I and partially He II p.e. spectra have been recorded for  $\text{EMe}_3\text{X}_2$  ( $\text{E} = \text{As}$  or  $\text{Sb}$ ,  $\text{X} = \text{F}$  or  $\text{Cl}$ ). The assigned He I  $\alpha$  p.e. spectra of  $\text{AsMe}_3\text{F}_2$ ,  $\text{AsMe}_3\text{Cl}_2$ ,  $\text{SbMe}_3\text{F}_2$ , and  $\text{SbMe}_3\text{Cl}_2$  are shown in Figure 1. Background spectra of  $\text{AsMeF}_2$ <sup>21</sup> and  $\text{AsMe}_3$ <sup>22</sup> are included for comparison. The He I  $\alpha$  p.e. spectrum of  $\text{SbMe}_4\text{F}$  is shown in Figure 2 and is correlated here with the p.e. spectrum of  $\text{SbMe}_5^1$  and with p.e. data for  $\text{SbMe}_3\text{F}_2$ . Vertical i.p.s determined at the band maxima are summarized in the Table.

All  $\text{EMe}_3\text{X}_2$  spectra (Figure 1) exhibit a characteristic band

Table. P.e. band maxima (vertical i.p.s in eV)

$\text{AsMe}_3\text{F}_2$	11.56, 12.08, 12.70, 13.71, 14.00, 15.11, 17.56, 18.15, 19.53 He II: 17.56, 18.07 (18.93), 19.45, 21.51
$\text{AsMe}_3\text{Cl}_2$	10.6, 12.35, 14.9
$\text{SbMe}_3\text{F}_2$	(10.98)/11.28, 11.80, 12.77, 13.59, 13.90, 14.48, 14.73 He II: 13.49, 14.50, 15.13, 17.77, 22.33
$\text{SbMe}_3\text{Cl}_2^1$	<i>ca.</i> 9.8(sh), 10.22, 10.65, 12.05, 14.65
$\text{SbMe}_4\text{F}$	9.15 [1], 10.84 [3], 12.44 [3], 14.3, 16.92 He II: 17.22, <i>ca.</i> 22.1
$\text{SbMe}_5^1$	7.36 [1], 10.5 [3], 13.2, 16.35, 18.25
$\text{AsMe}_3^{20}$	8.65, 10.7
$\text{SbMe}_3$	8.50, 10.05/10.48, 13.6
$\text{AsMeF}_2^{21}$	10.72, 13.68, 14.41, 16.00, 16.67
$\text{AsMe}_2\text{Cl}^{21}$	9.52, 10.82, 11.56, 12.21, 12.58, 13.5–16.1

sh = Shoulder. Numbers in square brackets refer to relative band intensities; values in parentheses are not unequivocally assigned; italicized numbers refer to mean values of complex bands.

pattern governed by the separation of  $n_{\text{X}}$  ( $n =$  non-bonding orbital),  $\sigma_{\text{E-R}}$  and C-H energy regions and the respective valence shell i.p.s of the atoms involved. The  $n_{\text{X}}$  region at low energies is identified by bands of high intensities with relatively small half-widths. At higher energies there is no doubt about the position of the C-H i.p.s (14 to *ca.* 16.5 eV) consisting of a broad featureless band. In contrast to the dichlorides [traces of decomposition products (*cf.* next section and Figure 1) could not be avoided for  $\text{AsMe}_3\text{Cl}_2$  during the sublimation procedure], the respective low-energy band groups are well resolved for both difluorides, nicely reflecting the band pattern with respect to the energy sequence, as expected and as calculated for  $\text{EH}_3\text{X}_2$  and  $\text{ER}_3\text{X}_2$ ,<sup>1,7,21a</sup> and as recently suggested for  $\text{PH}_3\text{F}_2$  by applying *ab initio* methods.<sup>7b</sup> It should be noted that both difluorides provide valuable reference material for the assignment of the complex p.e. spectra of the electron-rich Group 5 pentafluorides  $\text{VF}_5$ ,  $\text{PF}_5$ , and  $\text{AsF}_5$ .<sup>20</sup> To understand the i.p. patterns of the dihalides (Figure 1) as well as the band shifts that obviously occur on going from the parent  $\text{AsMe}_3$  to  $\text{AsMe}_3\text{X}_2$  and to elucidate the shapes of the m.o. types involved, model calculations on the basis of the SCC-X $\alpha$  approach<sup>8</sup> have been performed for the series  $\text{AsH}_3$ ,  $\text{AsH}_5$ ,  $\text{AsH}_3\text{F}_2$ . Orbital energies and the corresponding wavefunction plots are depicted in Figure 3.

Since C-H ionization energies appear well separated in all p.e. spectra reported for this class of compounds (*cf.* ref. 1), and particularly for the dichlorides, the problem of interpreting the p.e. data is actually reduced to the assignment for  $\text{EX}_2$  subunits or at least to the  $\text{EH}_3\text{X}_2$  prototypes. Therefore, the findings sketched in Figure 3 are apparently equally well suited to explain the low-energy p.e. band compositions of all the present compounds. For example,  $\text{AsMe}_3\text{F}_2$  is nicely simulated by  $\text{AsH}_3\text{F}_2$  despite the low energy of  $\sigma_{\text{As-C}}$ . Concerning the band distributions in Figure 1, some gross features are to be discussed before going into details: in agreement with the trend in the halogen atomic electronegativities, a band drift towards lower energies is observed on going from the fluorides to the corresponding dichlorides. This effect is less pronounced for the relatively remote C-H regions (Figure 1) as expected. However, on comparing the p.e. data for the parent trivalent  $\text{EMe}_3$  donors<sup>22</sup> with those of the dihalides (*cf.* ref. 1) (as outlined for the  $\text{AsMe}_3$ ,  $\text{AsMe}_3\text{Cl}_2$  pair in Figure 1), the  $\sigma_{\text{E-C}}$  ( $4e$ ) and C-H bands are both appreciably shifted towards higher energies (*ca.* 1.6 and *ca.* 1.4 eV, respectively) in accordance with the flow of charge from E to X upon oxidative addition of  $\text{X}_2$ . This is reflected by SCC-X $\alpha$  net atomic charges for the transition  $\text{AsH}_3 \rightarrow \text{AsH}_3\text{F}_2$  or  $\text{AsH}_5$ , respectively.

The  $\sigma_{\text{E-C}}$  energies are consequently attributed to the

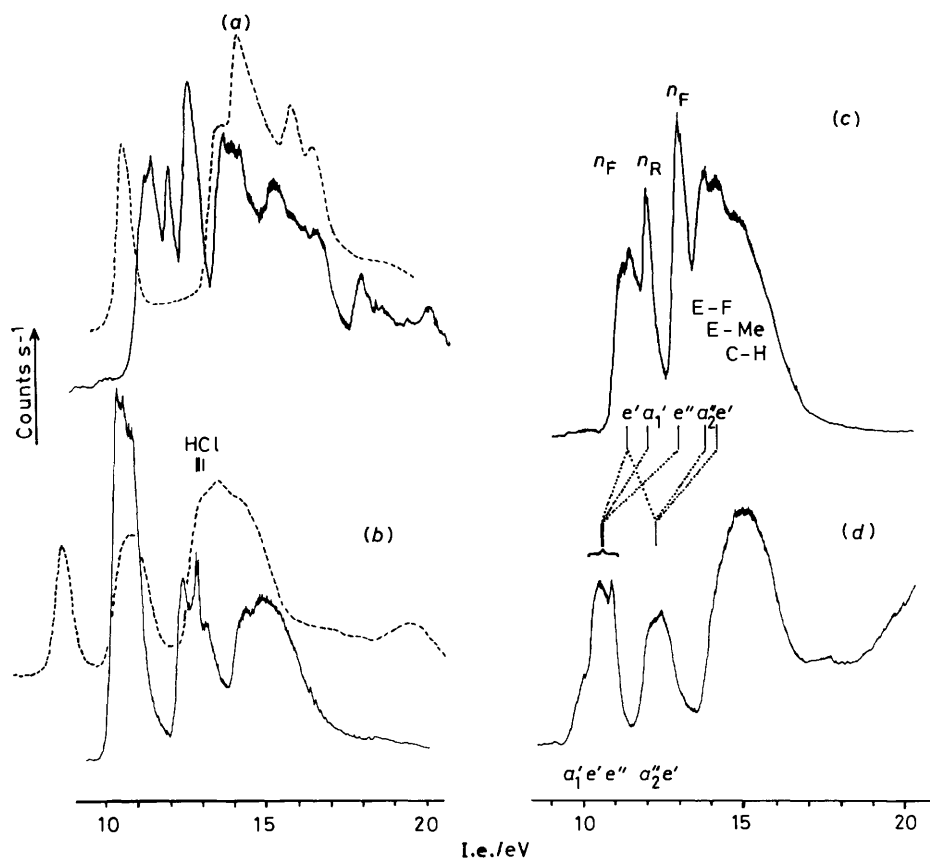


Figure 1. He I<sub>x</sub> photoelectron spectra of AsMe<sub>3</sub>F<sub>2</sub> (a), AsMe<sub>3</sub>Cl<sub>2</sub> (b), SbMe<sub>3</sub>F<sub>2</sub> (c), and SbMe<sub>3</sub>Cl<sub>2</sub> (d) with assignments for SbMe<sub>3</sub>Cl<sub>2</sub> according to the  $D_{3h}$  molecular point group. The background spectra (---) in (a) and (b) refer to AsMeF<sub>2</sub> and AsMe<sub>3</sub>

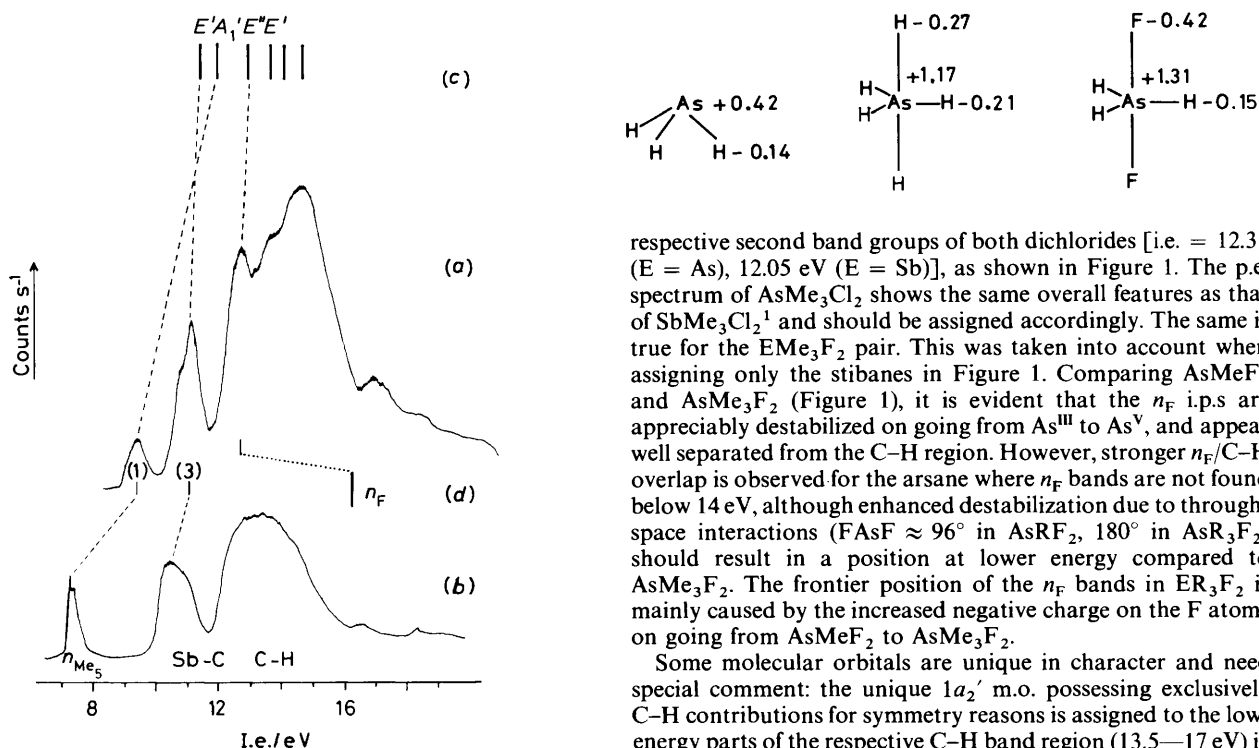


Figure 2. He I<sub>x</sub> photoelectron spectrum of SbMe<sub>4</sub>F (a) correlated with the i.p.s. of SbMe<sub>5</sub> (b), SbMe<sub>3</sub>F<sub>2</sub> (c), and HF (d)<sup>23</sup> to show the pronounced effect of successively replacing Me by F

respective second band groups of both dichlorides [i.e. = 12.35 (E = As), 12.05 eV (E = Sb)], as shown in Figure 1. The p.e. spectrum of AsMe<sub>3</sub>Cl<sub>2</sub> shows the same overall features as that of SbMe<sub>3</sub>Cl<sub>2</sub><sup>1</sup> and should be assigned accordingly. The same is true for the EMe<sub>3</sub>F<sub>2</sub> pair. This was taken into account when assigning only the stibanes in Figure 1. Comparing AsMeF<sub>2</sub> and AsMe<sub>3</sub>F<sub>2</sub> (Figure 1), it is evident that the n<sub>F</sub> i.p.s. are appreciably destabilized on going from As<sup>III</sup> to As<sup>V</sup>, and appear well separated from the C-H region. However, stronger n<sub>F</sub>/C-H overlap is observed for the arsane where n<sub>F</sub> bands are not found below 14 eV, although enhanced destabilization due to through-space interactions (FAsF ≈ 96° in AsRF<sub>2</sub>, 180° in AsR<sub>3</sub>F<sub>2</sub>) should result in a position at lower energy compared to AsMe<sub>3</sub>F<sub>2</sub>. The frontier position of the n<sub>F</sub> bands in ER<sub>3</sub>F<sub>2</sub> is mainly caused by the increased negative charge on the F atoms on going from AsMeF<sub>2</sub> to AsMe<sub>3</sub>F<sub>2</sub>.

Some molecular orbitals are unique in character and need special comment: the unique 1a<sub>2</sub>' m.o. possessing exclusively C-H contributions for symmetry reasons is assigned to the low-energy parts of the respective C-H band region (13.5–17 eV) in the p.e. spectra of EMe<sub>3</sub>X<sub>2</sub> because of its destabilizing Me-Me through-space interactions. This orbital could reflect the magnitude of the inductive effects exerted by the axial

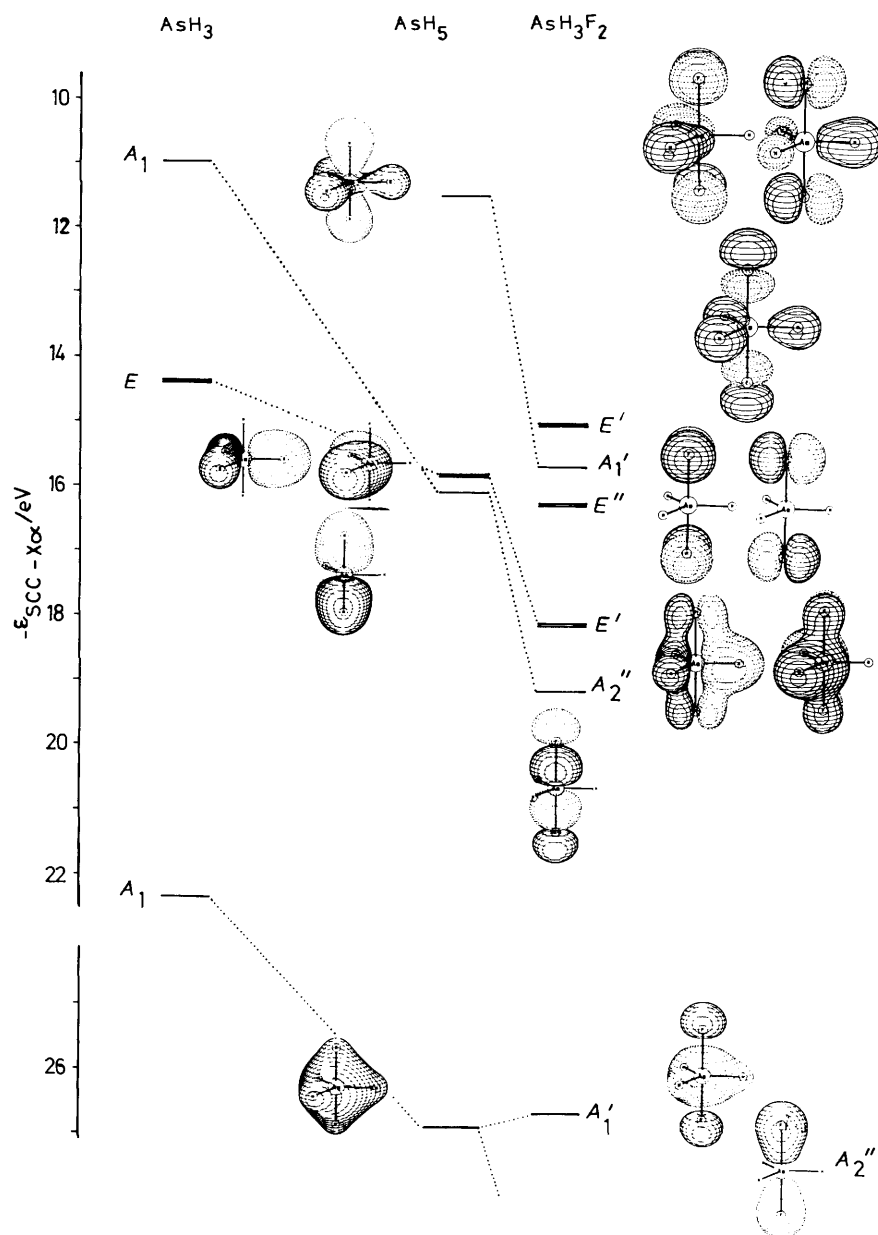


Figure 3. SCC-X $\alpha$  m.o. diagram ( $-\epsilon =$  orbital energy) for the transition  $\text{AsH}_3 \longrightarrow \text{AsH}_5 \longrightarrow \text{AsH}_3\text{F}_2$  with wavefunction plots; As  $d$  a.o.s are taken into account

substituents, but a corresponding p.e. peak is not resolved. This is analogous to the situation found for the  $\text{EMe}_3$  bases,<sup>22</sup> where this m.o. is subject to further enhanced through-space interactions for geometry reasons with respect to  $\text{EMe}_3\text{X}_2$ . As mentioned earlier, there is a low-energy  $a_1'$  component among the five occupied  $\sigma(\text{E-R})$  valence m.o.s which has to be attributed to the h.o.m.o. (i.e.  $i_1$  for  $\text{SbMe}_5^1$ ) or at least to the respective low-energy sections due to its non-bonding character. Not surprisingly, its energy depends strongly on the nature of the more negatively charged axial ligands. This  $a_1'$  m.o. is expected to be strongly stabilized by electronegative substituents occupying the apical positions, as simulated for  $\text{AsH}_5 \longrightarrow \text{AsH}_3\text{F}_2$  in Figure 3, and is assigned to the respective second i.p.s of the difluorides ( $E = \text{As}$ , 12.08 eV;  $E = \text{Sb}$ , 11.80 eV) for intensity reasons. Regarding the dichlorides, the respective  $a_1'$  bands are correspondingly attributed to the low-energy band groups [ $E = \text{As}$ , 10.6 eV;  $E = \text{Sb}$ , 10.2 eV (mean values)] but are not resolved. The low-energy shoulder at  $\approx 9.8$  eV for

$\text{SbMe}_3\text{Cl}_2$  could indicate that the  $a_1'$  band is at lowest energy and that the energy sequence for both dichlorides is reversed compared to the difluorides, i.e.  $|a_1' < e' < e''|$ . In the case of  $\text{SbMe}_4\text{F}$  (Figure 2) it is still ascribed to the first i.p. as for  $\text{SbMe}_5$ .<sup>1</sup> There is less correspondence between the former  $n_E$  lone-pair m.o. of the trimethyl donors  $\text{EMe}_3$ <sup>22</sup> and the low-energy  $a_2''$  m.o., which is strongly  $\sigma_{\text{E-X}}$  bonding for  $\text{ER}_n\text{X}_{5-n}$  compounds. The corresponding first\* and third bands of both difluorides may be assigned to ionizations from  $\pi$ -type  $n_F$  m.o.s as illustrated in Figure 3; they are directly related to the  $\pi$ -type m.o.s of the free halogens (i.p.<sub>1</sub> = 15.87 eV for  $\text{F}_2$ , = 11.6 eV for  $\text{Cl}_2$ ).<sup>12</sup> Both degenerate m.o.s may be classified with respect to the nodal plane stretched by the equatorial ligands: the symmetric  $n^+$  m.o. combination ( $e'$ ) is devoid of a central node

\* The first band of  $\text{AsMe}_3\text{F}_2$  is split due to spin-orbit splitting ( $\Delta i.p._1 = 0.14$  eV) and probably the Jahn-Teller effect.

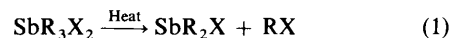
and contains appreciable or even predominant antibonding contributions from the E-C( $D_{3h}$ ) skeleton. Therefore, it is destabilized with respect to  $e''$ , the antisymmetric  $n$ -combination, which represents a nearly pure  $n_F$  non-bonding m.o. The bonding counterpart of the  $e'$  h.o.m.o. comprises  $\pi$ -type E-F bonding, besides appreciable  $n_F$  character and is localized at the low-energy edge of the C-H ionization region. This is clearly reflected by the p.e. spectra of both difluorides in Figure 1, which contain more information than those of the dichlorides. Both low-energy  $e'$  levels are nearly symmetrically split around the  $e''$  ionization potentials, as predicted by simple m.o. considerations.

Serial changes of elemental properties within a particular Group is often reflected by the spectroscopic properties of corresponding compounds, e.g. by band shifts. This is valid also for the p.e. spectral band patterns of such a series. The much larger energy gap between the valence-shell i.p.s of second-row atoms (including F), in contrast to the respective third-row atoms (including Cl) and heavier atoms within the same Group of the Periodic Table, is often not only followed by characteristic band shifts which may help to identify the pertinent m.o.s, but also by an interchange of correlation lines connecting i.p.s belonging to m.o.s of the same character (cf. the correlation lines for the series  $NMe_3 \times PMe_3 | AsMe_3 | SbMe_3 | BiMe_3$  or  $EMeF_2 \times EMeCl_2 | EMeBr_2 | EMeI_2$ , as cited in ref. 8b). Keeping this in mind one might wonder why the first i.p.s of  $EMe_3Cl_2$  are less shifted than the higher-energy  $n_X$ -based ones (i.e. i.p.<sub>2</sub>  $\rightarrow$   $\approx$  i.p.<sub>4</sub>) upon replacing the chlorines by fluorines. The reason might be that the h.o.m.o.s of both analogous  $EMe_3F_2$  compounds better compare with the  $\sigma_{E-C}$  bonding m.o.s; i.e. the second band groups of the dichlorides should preferably correlate with the respective first bands of the difluorides. This is fully consistent with both their relatively broad band widths and their fine structure. In this sense, the latter is best regarded as being caused mainly by spin-orbit splitting as found for the respective p.e. bands of quite a range of reference compounds (cf.  $\sigma_{E-C}$  bands of  $SbMe_3$  or  $BiMe_3$ <sup>8b</sup>). These considerations also form the basis for the assignment of the He I $\alpha$  p.e. spectrum of  $SbMe_4F$  (Figure 2). Here, there are three separate low-energy components at 9.15, 10.84, and 12.44 eV with an intensity pattern of (1:3:3), the third being partially superposed by C-H ionization energies. The first small band attributed to  $a_1'$  ( $n_{R_4F}$ ) is stabilized by  $\approx 1.8$  eV compared to  $SbMe_5$ .<sup>1</sup> The second i.p. corresponds mainly with the  $\sigma_{Sb-C}$  band of  $SbMe_5$ , centered at 10.5 eV, whereas the third probably originates from ionizations of the  $\pi$ -type  $n_F$  m.o.s. This is in accordance with simple m.o. applications starting from  $SbH_5$  and HF (i.p. = 16.16 eV)<sup>23</sup> in order to build up  $SbH_4F$ : the former  $\sigma_{Sb-H}$  energy region should be stabilized on replacing H by F, whereas the  $n_F$  band should be appreciably destabilized with respect to HF. The amount of  $\sigma_{Sb-C}$  stabilization is  $\approx 0.3$  eV with respect to  $SbMe_5$ ; the  $\Delta n_F$  destabilization amounts to  $\approx 3.7$  eV with respect to HF. The  $\sigma_{Sb-F}$  band is hidden underneath the C-H band complex.

The He II spectra recorded for the three fluorides do not show any spectacular intensity changes within the low-energy regions when compared to the respective He I spectra. Nevertheless, they provide some insight into the 15–25 eV region where i.p.s of typical  $s$ -type m.o.s (Sb, C) should appear. Since  $\sigma_{E-F}$  bands are not expected to occur at energies higher than those of e.g.  $EF_3$  (cf.  $AsF_3$  17.22, 17.82 eV and  $SbF_3$  16.06, 16.55 eV),<sup>8b</sup> the distinct high-energy features found for the three fluorides should together be ascribed to ionizations from "Sb + C"  $s$ -type m.o.s. One of these is illustrated for the parent  $AsH_3F_2$  at  $\approx 26.7$  eV in Figure 3 ( $2a_1'$ ,  $1a_2''$ , and  $1a_1'$  i.p.s are not expected to occur below 25 eV). The respective sharp  $2a_1'$  band for  $AsMe_3F_2$  can be identified at 21.5 eV by comparison with the He II spectral features of  $AsF_5$ .<sup>20</sup> Bands of enhanced intensity in the He II spectra between 17.5 and 17.8 eV (at 16.35 for  $SbMe_5$ ) are

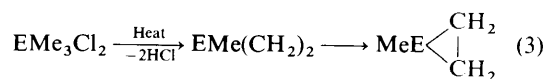
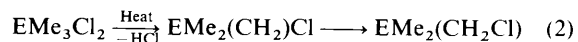
ascribed to Sb–Me, those between 18 and 21 eV to Sb–C  $s$ -type i.p.s.

*Variable-temperature Studies.*—Dihalogenostibanes  $SbR_3X_2$  have long been known as suitable precursors for  $SbR_2X$  (and indirectly also for  $SbRX_2$ ) which are formed by solid-state pyrolysis *in vacuo*,<sup>17,24</sup> according to equation (1). Formally, this



process may be regarded as a reductive elimination *via* least-motion loss of one axial (a) and one equatorial (e) ligand. The mode of the e/a departure has been a matter of debate<sup>2a,7</sup> as it is forbidden by symmetry,<sup>2a</sup> in contrast to the a/a and e/e alternatives. Concerning the thermally induced loss of methyl halides within the series  $SbMe_3X_2$  (X = F to I), one should note that reaction (1) proceeds most readily and with high yield in the case of the relatively unstable di-iodide, and becomes less facile on going towards the more electronegative halogens: only low yields are obtained with  $SbMe_3Cl_2$ , which may even be sublimed without decomposition under mild conditions. For generation of the fluorostibines  $SbR_2F$  this method is least appropriate. The difficulty in generating  $SbMe_2Cl$  in reasonable amounts on a preparative scale by cracking  $SbMe_3Cl_2$  at normal or reduced pressures does not contradict the predictions of the Woodward–Hoffmann rules applied to this particular problem.<sup>2a</sup> The reductive elimination of MeCl, which is generally expected and is experimentally utilized, is obviously depressed by side reactions and a high energy barrier.

This observation has inspired us to repeat this reaction under controlled conditions, i.e. where unimolecular decompositions are supposed to prevail. High-temperature u.v. photoelectron spectroscopy as well as high-temperature f.i. mass spectrometry were employed for analysis. The compounds chosen were  $AsMe_3Cl_2$  and  $SbMe_3Cl_2$ . As exemplified by the less stable arsorane in Figure 4, both compounds first lose HCl when heated under vacuum. The temperatures quoted in Figure 4 refer to those of the pyrolysis tube and are certainly much higher than the actual temperatures reached by the sample vapour.<sup>25</sup> As already shown in Figure 1, by the small HCl peaks at 12.66 eV ( $n_{Cl} 1\pi$ ),<sup>23</sup>  $AsMe_3Cl_2$  could not even be sublimed from the sample reservoir without any decomposition. A trace of MeCl occurs only above 1 000 K (i.p. at 11.25 eV) as indicated by the spectrum at 1 155 K (Figure 4). The p.e. spectrum of the presumed pyrolysis product  $AsMe_2Cl$ <sup>21</sup> (dotted line, Figure 4) is presented to demonstrate that this compound is *not* produced during gas-phase thermolysis of  $AsMe_3Cl_2$ . Only HCl loss was observed for the surprisingly stable stibane at tube temperatures between 1 400 and 1 600 K. In both cases, at least one new band was detected, i.e. a low-energy hump centred at 8.9 eV for the  $AsMe_3Cl_2$  and at 8.8 eV for the  $SbMe_3Cl_2$  pyrolyzates, respectively. These p.e. bands obviously do *not* belong to those of the respective  $EMe_2Cl$  species nor to MeCl or the methyl radical. Whether they indicate the commencement of formation of the  $EMe_3$  molecules as identified also by f.i. mass spectrometry cannot be solved at present. Of the two possible unimolecular fragmentation pathways (2) and (3), as suggested



by the variable-temperature p.e. results, only (2) is in accordance with the respective f.i. mass spectrometric results (see below). Furthermore, a  $E^V \rightarrow E^{III}$  rearrangement according to equation (3) was recently reported by Appel *et al.*<sup>26</sup> Whether

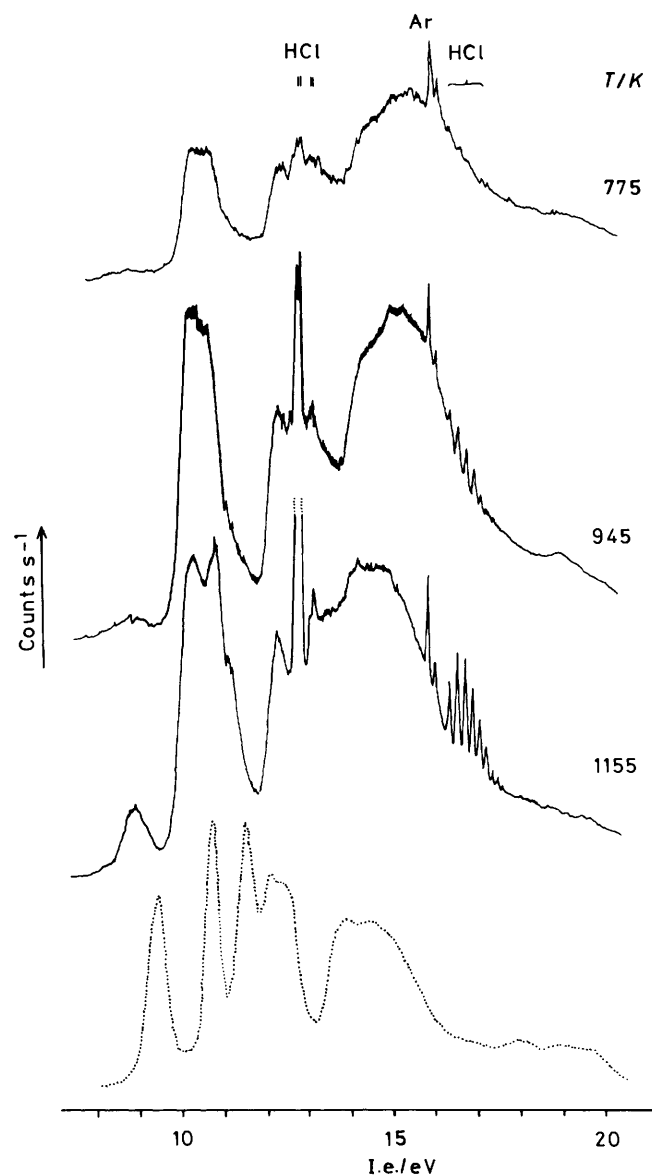


Figure 4. Photoelectron spectra recorded upon gas-phase pyrolysis of  $\text{AsMe}_3\text{Cl}_2$ ; the temperatures quoted refer to those of the pyrolysis tube; (···)  $\text{AsMe}_2\text{Cl}$

the new low-energy bands occurring upon pyrolysis belong to the final, and thermodynamically more stable, product  $\text{EMe}_2(\text{CH}_2\text{Cl})$  cannot be decided due to strong p.e. band superposition; nevertheless it is a reasonable assumption, since a value of 8.9 eV found for the arsorane pyrolyzate seems to be too high with respect to  $\text{AsMe}_3(\text{CH}_2)$  (i.p.<sub>1</sub> = 6.72 eV)<sup>27</sup> to be acceptable as the first i.p. of  $\text{AsMe}_2(\text{CH}_2)\text{Cl}$ . Furthermore the collision-activation mass spectrum of the e.i. induced peak at  $m/z$  154, formed pyrolytically from  $\text{AsMe}_3\text{Cl}_2$  (cf. Figure 8), exhibits a dominant peak at  $m/z$  105, corresponding to loss of  $\text{CH}_2\text{Cl}^\cdot$ , which is indicative of the  $\text{AsMe}_2(\text{CH}_2)\text{Cl}$  structure.

Because of the reaction conditions chosen for the u.v.p.e. and f.i. mass spectrometric experiments, surface-promoted reactions can be excluded. Unimolecular thermal degradation of both dichlorides apparently does not proceed *via* the thermally forbidden loss of the *a/e* ligands as is generally assumed by experimentalists. Loss of  $\text{MeX}$  as observed experimentally could also be caused by intermolecular formation of  $\text{EMe}_2\text{X}$ .

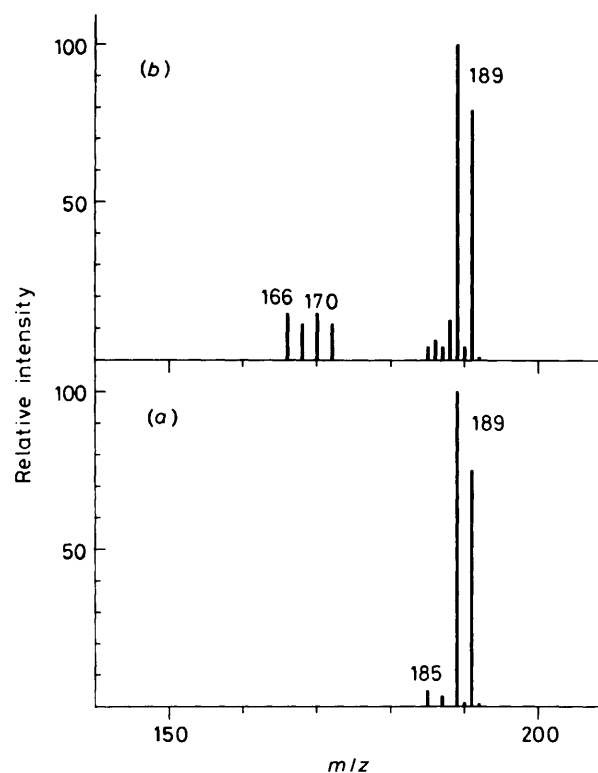


Figure 5. Field ionization mass spectra of (a)  $\text{SbMe}_3\text{F}_2$  and (b) following pyrolysis at 1 043 K

Generation of  $\text{HCl}$  instead of  $\text{MeCl}$  is also observed in the p.e. spectrum when the involatile  $\text{PMe}_3\text{Cl}_2$  analogue is heated *in vacuo*; this case is somewhat more complex, since reactions of higher order have to be considered wherever solid-state pyrolysis is applied. The results for  $\text{PMe}_3\text{Cl}_2$  are not conclusive at the present stage of investigation and will be presented in conjunction with pyrolysis experiments and matrix-isolation investigations using  $\text{PH}_3\text{F}_2$ ,  $\text{SbMe}_2\text{Cl}_3$ ,  $\text{EMe}_4\text{X}$ ,  $\text{NbMe}_3\text{Cl}_2$ , and  $\text{TaMe}_3\text{Cl}_2$  precursors and derivatives. It should be mentioned that the involatile (ionic) species  $\text{AsMe}_4\text{Cl}$  and  $\text{SbMe}_4(\text{CN})$  both eliminate  $\text{MeX}$  instead of  $\text{HX}$  when heated under vacuum. The same is true for  $\text{AsMe}_3\text{Br}_2$ .

Analysis of the pyrolytic decomposition of  $\text{EMe}_3\text{X}_2$  by f.i. mass spectrometry strongly supported the idea of a thermally induced elimination of  $\text{HX}$ .

It should be noted that neither the arsoranes  $\text{AsMe}_3\text{X}_2$  nor the stibanes  $\text{SbMe}_3\text{X}_2$  exhibit molecular ions under f.i. mass spectrometric conditions.\* The fluorine-substituted species typically exhibit  $M - 15$  as the ion at highest mass, whereas the chlorine-substituted analogues exhibit  $M - \text{Cl}$  as the predominant ion,  $M - 15$  having only very low intensities.

As mentioned above, the fluoro compounds appeared rather stable, and only minor thermal decompositions were observed. Pyrolysis (1 043 K) of  $\text{SbMe}_3\text{F}_2$  gave rise to some formation of  $\text{SbMe}_3$  ( $m/z$  166, 168) and  $\text{SbMe}_2\text{F}$  ( $m/z$  170, 172), the latter being formed by elimination of  $\text{MeF}$  (Figure 5). No  $\text{HF}$  elimination, which should result in the appearance of a set of

\* In principle, f.i. mass spectrometry gives rise only to molecular ions, however in some cases abundant fragment ions, in general due to field-induced fragmentation, *i.e.* simple bond fission, are observed (H. D. Beckey, 'Principles of Field Ionization and Field Desorption Mass Spectrometry,' Pergamon, New York, 1977).

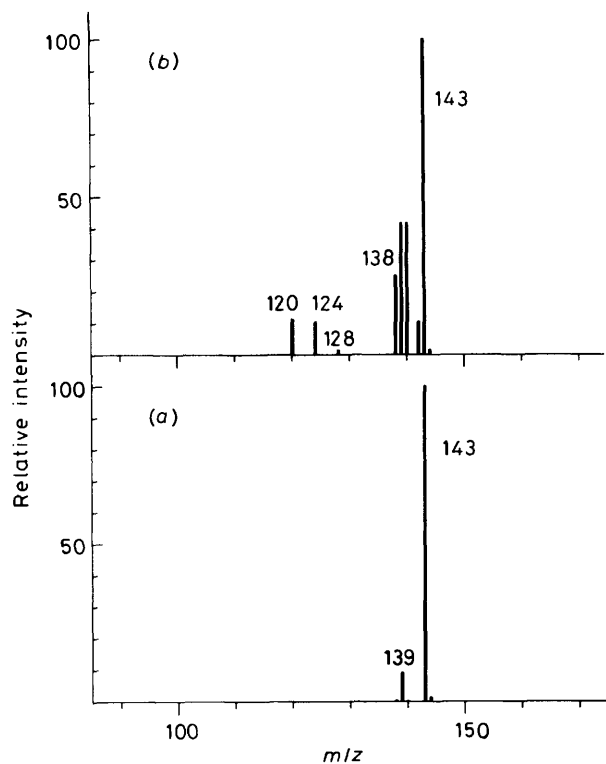


Figure 6. Field ionization mass spectra of (a)  $\text{AsMe}_3\text{F}_2$  and (b) following pyrolysis at 1043 K

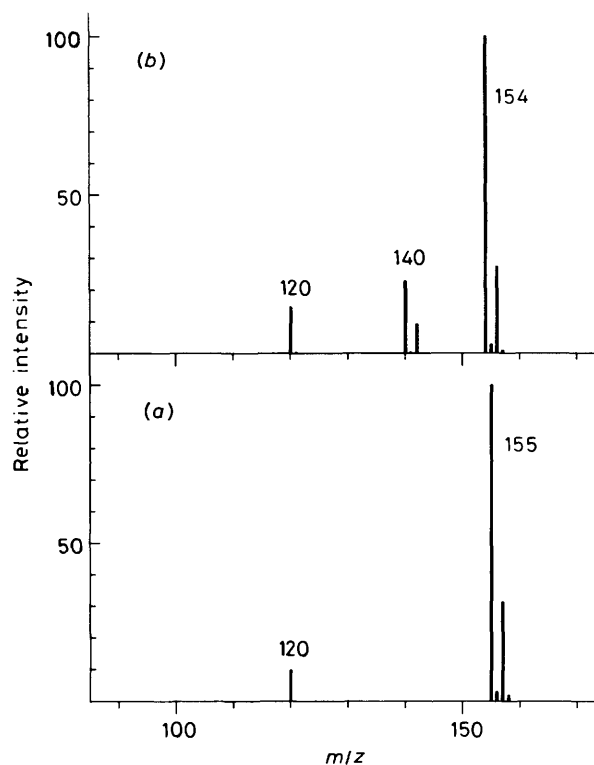


Figure 8. Field ionization mass spectra of (a)  $\text{AsMe}_3\text{Cl}_2$  and (b) following pyrolysis at 1043 K

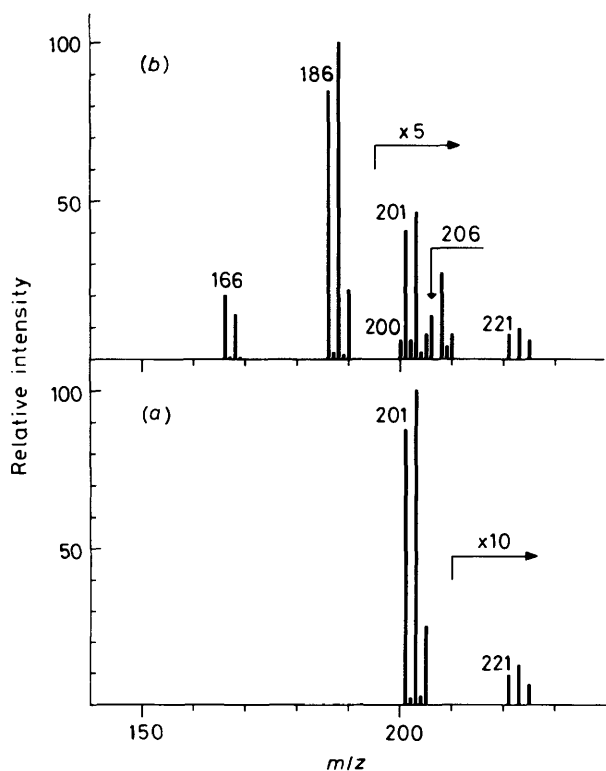


Figure 7. Field ionization mass spectra of (a)  $\text{SbMe}_3\text{Cl}_2$  and (b) following pyrolysis at 1043 K

ions at  $m/z$  184, 186, was noted. The corresponding arsorane,  $\text{AsMe}_3\text{F}_2$ , was found to be somewhat more thermally labile. Pyrolysis (1043 K) afforded ions at  $m/z$  138, 128, 124, and 120 assigned to  $\text{AsMe}_2(\text{CH}_2)\text{F}$ ,  $\text{AsMe}_2\text{F}$ ,  $\text{AsMe}_2\text{F}$ , and  $\text{AsMe}_3$ , respectively (Figure 6). In addition, a relative increase in intensity at  $m/z$  139, corresponding to loss of F, could be observed (Figure 6).

A similar relative lability to that of the fluorine-substituted arsorane and stibane was observed for the chlorine-substituted compounds,  $\text{SbMe}_3\text{Cl}_2$  and  $\text{AsMe}_3\text{Cl}_2$ . Pyrolysis of  $\text{SbMe}_3\text{Cl}_2$  (1043 K) unambiguously revealed  $\text{SbMe}_2\text{Cl}$  ( $m/z$  186, 188, and 190) as the major product, in addition to  $\text{SbMe}_3$  ( $m/z$  166 and 168) and  $\text{SbMeCl}_2$  ( $m/z$  206, 208, and 210) (Figure 7). However, inspection of the cluster at around  $m/z$  201, 203, and 205 before and after pyrolysis (*cf.* Figure 7) nicely demonstrated the appearance of a new set of ions ( $m/z$  200, 202, and 204), which can be ascribed to ' $\text{SbMe}_2(\text{CH}_2)\text{Cl}$ '. In the pyrolysis of  $\text{AsMe}_3\text{Cl}_2$  (Figure 8) it was unambiguously demonstrated that ' $\text{AsMe}_2(\text{CH}_2)\text{Cl}$ ' ( $m/z$  154 and 156) was the predominant pyrolysis product. In addition some  $\text{AsMe}_2\text{Cl}$  ( $m/z$  140 and 142) and  $\text{AsMe}_3$  ( $m/z$  120) could be observed (Figure 8).

Concerning the solid-state pyrolysis of the fluorine- and chlorine-substituted arsoranes and stibanes  $\text{EMe}_3\text{X}_2$  ( $\text{E} = \text{As}$  or  $\text{Sb}$ ,  $\text{X} = \text{F}$  or  $\text{Cl}$ ), we conclude, based on the combined p.e. and f.i. mass spectrometric investigations, that (a) the arsoranes are significantly more labile than the corresponding stibanes, and (b) the chlorine-substituted species are more labile than the fluorine analogues. Hence, loss of  $\text{HX}$  was observed for  $\text{AsMe}_3\text{Cl}_2$ ,  $\text{SbMe}_3\text{Cl}_2$ , and  $\text{AsMe}_3\text{F}_2$ , but not for  $\text{SbMe}_3\text{F}_2$ . In all cases studied,  $\text{EMe}_3$  and  $\text{EMe}_2\text{X}$  ( $\text{MeX}$  extrusion) were formed.

Finally,  $\text{SbMe}_4\text{F}$  was pyrolyzed in the temperature range 1043–1404 K. The only product observed was  $\text{SbMe}_3$ ,

corresponding to elimination of fluoromethane, in accordance with p.e. spectroscopic analysis of the pyrolyzate.

### Acknowledgements

This work was supported by the Deutsche Forschungsgemeinschaft. S. E. thanks her co-workers Dr. Horst Walther and Jens Kudnig for handling the computer software used, and Dr. M. Grodzicki for providing the SCC-X $\alpha$  program and helpful discussions. Technical assistance by H. J. Lempka is gratefully acknowledged.

### References

- 1 S. Elbel and H. tom Dieck, *Z. Anorg. Allg. Chem.*, 1981, **483**, 33.
- 2 (a) R. Hoffmann, J. M. Howell, and E. L. Muettterties, *J. Am. Chem. Soc.*, 1972, **94**, 3047; (b) R. R. Holmes, *Acc. Chem. Res.*, 1972, **5**, 296.
- 3 (a) G. Trinquier, J.-P. Daudey, G. Caruana, and Y. Madaule, *J. Am. Chem. Soc.*, 1984, **106**, 4794; (b) J. M. Howell, *ibid.*, p. 3745.
- 4 A. Strich, *Inorg. Chem.*, 1978, **17**, 942; J. A. Altmann, K. Yates, and I. G. Csizmadia, *J. Am. Chem. Soc.*, 1976, **98**, 1450.
- 5 W. J. Kutzelnigg, *J. Chim. Phys. Phys.-Chim. Biol.*, 1981, **78**, 295; J. I. Musher, *Angew. Chem.*, 1969, **81**, 68; J. M. Howell, *J. Am. Chem. Soc.*, 1975, **97**, 3930; T. A. Halgren, L. D. Brown, D. A. Kleiner, and W. N. Lipscomb, *ibid.*, 1977, **99**, 7441.
- 6 H. J. Bestmann, J. Chandrasekhar, W. G. Downey, and P. von R. Schleyer, *J. Chem. Soc., Chem. Commun.*, 1980, 978.
- 7 (a) W. J. Kutzelnigg and J. Wasilewski, *J. Am. Chem. Soc.*, 1982, **104**, 953; (b) F. Keil and W. Kutzelnigg, *ibid.*, 1975, **97**, 3623 and refs. therein; (c) A. Rauk, L. C. Allen, and K. Mislow, *ibid.*, 1972, **94**, 3035; (d) J. M. Howell, *ibid.*, 1977, **99**, 7447.
- 8 (a) M. Grodzicki, *J. Phys. B*, 1980, **13**, 2683; (b) M. Grodzicki, H. Walther, and S. Elbel, *Z. Naturforsch., Teil B*, 1984, **39**, 1319.
- 9 L. Carlsen and H. Egsgaard, *Thermochim. Acta*, 1980, **38**, 47; H. Egsgaard, E. Larsen, and L. Carlsen, *J. Anal. Appl. Pyrol.*, 1982, **4**, 23.
- 10 H. Egsgaard and L. Carlsen, *J. Anal. Appl. Pyrol.*, 1983, **5**, 1.
- 11 S. Elbel, H. tom Dieck, H. Walther, and J. Krizek, *Inorg. Chim. Acta*, 1981, **53**, L101; J. M. Dyke, S. Elbel, A. Morris, and J. C. H. Stevens, *J. Chem. Soc., Faraday Trans. 2*, 1986, 637.
- 12 A. W. Potts and W. C. Price, *Trans. Faraday Soc.*, 1971, **581**, 1242; G. Bieri, *J. Electron Spectrosc.*, 1981, **23**, 281.
- 13 L. Verdonck and G. P. van der Kelen, *Spectrochim. Acta, Part A*, 1977, **33**, 601.
- 14 W. L. Jorgensen, *Quantum Chem. Program Exchange*, 1977, **12**, 340.
- 15 G. G. Long, G. O. Doak, and L. D. Freedman, *J. Am. Chem. Soc.*, 1964, **86**, 209.
- 16 G. T. Morgan and G. R. Davies, *Proc. R. Soc. London, Ser. A*, 1926, **110**, 523; H. Landholt, *J. Prakt. Chem.*, 1961, **84**, 328.
- 17 S. Samaan, in 'Methoden der Organischen Chemie,' ed. E. Müller, G. Thieme Verlag, Stuttgart, 1978, vol. 13, pp. 351, 537 and refs. therein.
- 18 M. N. O'Brian, G. O. Doak, and G. G. Long, *Inorg. Chim. Acta*, 1967, **1**, 34.
- 19 B. M. Gimarc, *J. Am. Chem. Soc.*, 1978, **100**, 2346.
- 20 (a) G. Rüniger, Diploma Thesis, University of Hamburg, 1985; (b) S. Elbel, M. Grodzicki, J. Kudnig, and G. Rüniger, *Organometallics*, submitted for publication.
- 21 (a) H. Walther, Phil.D. Thesis, Hamburg, 1983; (b) S. Elbel and H. Walther, *J. Mol. Spectrosc.*, submitted for publication.
- 22 S. Elbel, H. Bergmann, and W. Ensslin, *J. Chem. Soc., Faraday Trans. 2*, 1974, 555.
- 23 D. W. Turner, C. Baker, A. D. Baker, and C. R. Brundle, *Molecular Photoelectron Spectroscopy*, Wiley-Interscience, New York, 1970; W. v. Niessen, L. S. Cederbaum, W. Domcke, and G. H. F. Dierksen, *Chem. Phys.*, 1981, **56**, 43.
- 24 M. Wieber, D. Wirth, and I. Fetzter, *Z. Anorg. Allg. Chem.*, 1983, **505**, 134 and refs. therein.
- 25 See, for example, H. Egsgaard, P. Bo, and L. Carlsen, *J. Anal. Appl. Pyrol.*, 1985, **8**, 3.
- 26 R. Appel, T. Gaitzsch, and F. Knoch, *Angew. Chem.*, 1985, **97**, 421.
- 27 K.-H. A. Ostojka Starzewski, W. Richter, and H. Schmidbaur, *Chem. Ber.*, 1976, **109**, 473.

Received 9th December 1985; Paper 5/2148